Int J Thermophys (2010) 31:1583–1598
DOI 10.1007/s10765-010-0801-1

"Disappearing Object" Radiation Thermometer for Low-Emissivity Process Control

P. Saunders · D. R. White

Received: 1 April 2010 / Accepted: 17 July 2010 / Published online: 30 July 2010
© Springer Science+Business Media, LLC 2010

Abstract One of the long-standing problems in metals-processing industries is the measurement of the temperature of low-emissivity targets. Such measurements are typically accompanied by problems with reflections and highly variable emissivity, so conventional spectral-band radiation thermometry is subject to large errors and uncertainties. This article presents the design principles of a novel radiation thermometer that places the target inside a blackbody cavity at the desired process temperature. Uncertainties in the measurements of target temperature due to reflections and the target emissivity fall in proportion to the difference between the target and process temperatures, and are minimized when the target is at the desired process temperature. This procedure enables accurate control of the process to a level near the minimum uncertainty, which is lower than those for other current measurement techniques. The article presents the uncertainty analysis for the new thermometer, and suggests practical realizations for applications in aluminum extrusion plants and steel strip mills.

Keywords Aluminum extrusion · Galvannealing · Low emissivity · Metals processing · Radiation thermometry

1 Introduction

The application of radiation thermometry to industrial temperature measurement is subject to many problems that are often insignificant in laboratory applications. Two of the major problems relate to the unknown emissivity of industrial materials and

P. Saunders (✉) · D. R. White
Measurement Standards Laboratory of New Zealand, Industrial Research Ltd, PO Box 31-310, Lower Hutt, New Zealand
e-mail: p.saunders@irl.cri.nz

to the reflection of radiation from hot objects in the vicinity of the target of interest. These problems are exacerbated in metals-processing industries where material emissivities are low and often highly variable. Examples include the monitoring of aluminum extrusion and steel strip in galvanizing processes, both of which exhibit large relative variations in the target emissivity and have relatively tight temperature requirements. Despite the existence of these problems, which lead to large uncertainties, radiation thermometry is still the preferred temperature measurement technique because the environments are often hostile to most types of contact thermometers and the targets are often moving.

Current measurement methods that have achieved a reasonable level of success in these industries attempt to minimize the influence of emissivity through emissivity enhancement using multiple reflections [1,2] in the manner of the gold-cup pyrometer [3]; through the utilization of naturally occurring quasi-blackbody cavities, such as the wedge formed between the strip and a roller in the steel industry [4,5]; or by the implementation of dual- or multi-wavelength pyrometers [6].

In contrast, this article proposes a novel type of radiation thermometer that exploits blackbody principles to minimize the dependence of the measured temperature on emissivity and to control the reflected radiation. By enclosing the target object inside a blackbody cavity at the desired process temperature, the target's temperature can be inferred from the difference between the temperatures obtained from the target and the blackbody. The minimum uncertainty occurs when the temperature difference is zero and the target is at the correct temperature. By analogy with the disappearing filament pyrometer, the object can be said to "disappear" into the blackbody background, and so the device is described as a "disappearing object" radiation thermometer.

The article begins with a brief discussion of the principles of radiation thermometry relevant to this problem, and then quantifies the typical measurement uncertainties achievable using a range of current radiation thermometry techniques: conventional radiation thermometry, dual and multi-wavelength thermometry, and gold-cup thermometry. The disappearing object thermometer is then described, and the measurement uncertainties are analyzed based on its design principles. The article finishes with a comparison of these uncertainties with the uncertainties that arise using the existing techniques, and some concluding remarks are given. All uncertainties quoted in this article are standard uncertainties.

2 General Principles

Radiation thermometers infer the temperature of a target from a measurement of its spectral radiance integrated over the operating bandwidth of the thermometer. For the sake of clarity, it will be assumed here that the bandwidth is sufficiently narrow and the thermometer can be treated as monochromatic. The conclusions presented are equally valid when extended to finite bandwidths. The spectral radiance of an object is generally comprised two components: a component due to self-emission of radiation and a component due to reflection of radiation from the surroundings [7],

$$L_{\mathrm{m}} = \varepsilon(\lambda) L_{\mathrm{b}}(\lambda, T_{\mathrm{s}}) + [1 - \varepsilon(\lambda)]\, L_{\mathrm{b}}(\lambda, T_{\mathrm{w}}). \tag{1}$$

Here, L_m is the spectral radiance measured by the thermometer, $L_b(\lambda, T)$ is the spectral radiance of a blackbody at wavelength λ and temperature T, given by Planck's law, T_w is a weighted average radiance temperature of the surroundings, T_s is the true temperature of the target, and $\varepsilon(\lambda)$ is its spectral emissivity. In Eq. 1, it is assumed that the target is opaque and that its reflectance, assumed to be diffuse, is equal to $1-\varepsilon(\lambda)$.

The task of the radiation thermometer is to somehow infer the value of T_s from the measurement of L_m. Clearly, if all the parameters in Eq. 1 are fully known, then it is a simple algebraic exercise to rearrange the equation to yield T_s as the subject. However, in an industrial environment, the values of $\varepsilon(\lambda)$ and T_w generally change from one measurement to another, so unless it is convenient to measure these values each time a temperature is required, this approach is not practicable.

The emissivity of a material generally depends upon surface roughness, degree of oxidation, viewing angle, and wavelength. For example, in the aluminum extrusion industry, the emissivity of the aluminum may be in the range from 0.05 to 0.3 [8] depending on the alloy type, degree of oxidation, and wavelength. Determining the temperature of the extrusion just after it leaves the die is critical for controlling the extrusion speed in order to minimize the formation of defects in the extruded product. In the galvanneal process, in which zinc-coated steel is heat-treated to produce a zinc-rich intermetallic layer on the strip surface, the emissivity varies from 0.1 for the pure zinc liquid to 0.8 for the fully alloyed layer [9]. The annealing temperature and annealing time determine the properties of the final product, hence the temperature must be known accurately.

Evaluation of the average radiance temperature of the surroundings, T_w in Eq. 1, is usually a complex process [10]. It is obtained by determining the radiance of each surface in the entire hemisphere above the measurement spot on the target of interest (including distant ambient surfaces), performing a weighted average of these radiances, and then inferring the radiance temperature corresponding to this average radiance. The weights used in the averaging process are determined from the geometric view factors [11] (also called configuration factors) of each surface as seen from the measurement spot. As implied by Eq. 1, the actual measurement geometry is equivalent to completely enclosing the target spot with a blackbody whose true temperature is T_w.

Before describing how the proposed new thermometer can overcome the problems of variable low emissivity and reflections, several of the different approaches currently employed to solve Eq. 1 are reviewed, and their typical errors and uncertainties are presented.

2.1 Conventional Radiation Thermometry

In conventional radiation thermometry, the term in Eq. 1 corresponding to the reflected radiation is neglected, and the measurement is performed by compensating for emissivity only. This is done by simply adjusting an instrumental emissivity setting on the device to a previously determined value of $\varepsilon(\lambda)$. Figure 1 shows the error using this approach for thermometers operating at different wavelengths for an example in the aluminum extrusion industry, where it is assumed that the emissivity of aluminum is 0.2 (at each wavelength) and the true temperature is 520 °C. For a typical aluminum

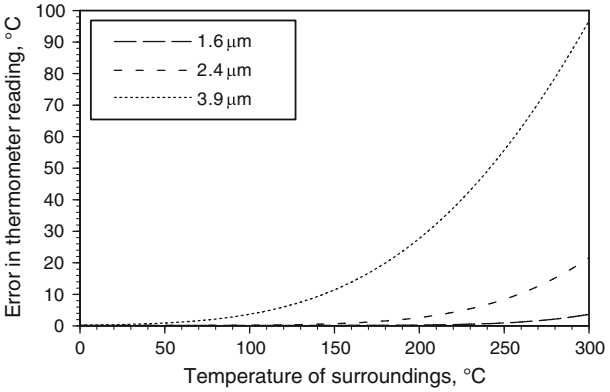

Fig. 1 Error in thermometer reading due to reflections for spectral-band radiation thermometers operating at three different wavelengths viewing a target with an emissivity of $\varepsilon(\lambda) = 0.2$ at a temperature of $T_s = 520\,°C$, where the instrumental emissivity is set to $\varepsilon_{instr} = 0.2$

extrusion press, the surroundings (the throat of the press) may have a temperature near 60 °C, so that for a 1.6 μm or 2.4 μm thermometer, the error would be negligible, while for a 3.9 μm thermometer, the error would only be about 1 °C.

While the measurement errors due to reflections are tolerable, problems arise when the uncertainties are considered. Because of the low emissivity of aluminum, the uncertainty in the measured temperature is dominated by the uncertainty in emissivity [12], and is approximated by

$$u_{T_m} = \frac{\lambda T_s^2}{c_2} \frac{u_\varepsilon}{\varepsilon}, \tag{2}$$

where c_2 is the second radiation constant. Assuming that the emissivity may be anywhere in the range from 0.1 to 0.3 due to different alloy compositions ($u_\varepsilon = 0.06$, one-sigma value for a rectangular distribution), then the standard uncertainty is 21 °C, 31 °C, or 51 °C for a 1.6 μm, 2.4 μm, or 3.9 μm thermometer, respectively. A smaller additional uncertainty, typically 1 °C, will also arise in the measurement of the target radiance itself.

For applications where the background temperature is considerably higher than the 60 °C of the above example, such as in the galvannealing process where it may be as high as 600 °C, reflection errors are significant. These reflection errors can be compensated for by making a separate measurement of the weighted average radiance temperature, T_w, and solving Eq. 1 for T_s. However, except for a narrow range of T_w values close to T_s, the uncertainty due to emissivity is still a limitation for low-emissivity materials.

2.2 Ratio Thermometry

Ratio thermometers attempt to overcome the problem of unknown or variable emissivity by inferring the temperature of the target from the ratio of radiance measurements

made at two different wavelengths. So long as the emissivity is the same at the two wavelengths (and reflections are negligible), the measurement is independent of the value of the emissivity. However, this is rarely the case for metals. When the metal surface is relatively free of oxide, its emissivity is a direct function of the electrical conductivity of the metal, meaning that the emissivity is proportional to the reciprocal of the square root of wavelength [13]. In this case, and in the absence of reflections, the measured temperature, T_m, is governed by the equation,

$$\frac{L_b(\lambda_1, T_m)}{L_b(\lambda_2, T_m)} = \left(\frac{\lambda_2}{\lambda_1}\right)^{1/2} \frac{L_b(\lambda_1, T_s)}{L_b(\lambda_2, T_s)}, \tag{3}$$

where λ_1 and λ_2 are the two operating wavelengths. Thus, application of a ratio thermometer operating at 1.6 μm and 1.8 μm to such a target would lead to an error, $T_m - T_s$, close to 40 °C when the target is at $T_s = 520$ °C. The error would be even larger for a pair of longer wavelengths, and the presence of any reflected radiation would lead to still larger error [14].

In principle, it is possible to compensate for a known wavelength dependence of emissivity by using a ratio thermometer with an "emissivity slope" adjustment. For the case where the emissivity is exactly proportional to the inverse of the square root of wavelength, an emissivity slope equal to the square root of the ratio of the operating wavelengths would be appropriate. However, any slight variations from this exact emissivity dependence would give rise to relatively large errors. The temperature error for a ratio thermometer scales as

$$\Delta T_m = \frac{\lambda_1 \lambda_2}{\lambda_1 - \lambda_2} \frac{T_s^2}{c_2} \frac{\Delta \varepsilon_r}{\varepsilon_r}, \tag{4}$$

where ε_r is the ratio of emissivities at λ_1 and λ_2, and $\Delta\varepsilon_r$ is the error in the applied emissivity slope. Comparing Eq. 4 with Eq. 2, it can be seen that the ratio thermometer behaves like a single-wavelength spectral-band thermometer with an operating wavelength of $\Lambda = \lambda_1\lambda_2/(\lambda_1 - \lambda_2)$. For example, for $\lambda_1 = 1.6$ μm and $\lambda_2 = 1.8$ μm, the value of Λ is 14.4 μm. In effect, the thermometer trades the need to know absolute emissivity at a single wavelength for a need to know the ratio of emissivities at two wavelengths, but at the expense of a much increased sensitivity to this emissivity ratio.

Emissivity compensation algorithms, more sophisticated than a simple ratio, can be employed based on prior measurements of emissivity at the two operating wavelengths for specific alloy compositions under various conditions. In effect, the thermometer is "tuned" for one particular alloy. However, for the galvanneal process, for example, measurements based on these algorithms seem to be limited to an uncertainty of about 20 °C [9]. Reflected radiation, additionally, introduces relatively large errors.

2.3 Multi-Wavelength Thermometry

By increasing the number of wavelengths available in a radiation thermometer, it is possible to take a sufficient number of measurements to include a model for the

wavelength dependence of emissivity, of arbitrary sophistication, in the thermometer's measurement algorithm. Thus, a multi-wavelength thermometer might be expected, in principle, to be able to measure both the temperature and emissivity of a surface of any unknown emissivity. However, the sensitivity of these thermometers to uncertainties in the measured radiances increases almost exponentially as the number of wavelengths increases [14,15]. In practice, the sensitivity of multi-wavelength thermometers to the target temperature is so low that the thermometer is virtually useless, with uncertainties often as large as 100 °C or more. Such thermometers are also intolerant of reflections [14].

As with the dual-wavelength thermometers exploiting known emissivity relationships, by building additional information into multi-wavelength thermometers, it is possible to constrain the multi-wavelength algorithm and decrease its sensitivity to uncertainty. One method is to use measurements at two wavelengths as described above for ratio thermometry, and a measurement at a third wavelength to identify the particular alloy. The accuracy of such devices is expected to be similar to that of "tuned" ratio thermometers, and thus around 20 °C.

2.4 Gold-Cup Thermometry

The gold-cup pyrometer [3] is sometimes used for industrial temperature measurements where emissivity and reflection errors are problematic. The device consists of a small gold-plated hemisphere with a small window at the top through which radiation can pass onto a detector. In use, the hemisphere is mounted on a long steel pole and placed up against the surface of interest, blocking out any radiation from the surroundings. Inter-reflections between the inside of the cup and the target surface increase the effective emissivity of the surface to an amount given by [10]

$$\varepsilon_{\text{eff}} = 1 - \frac{(1-\rho_{\text{g}})(1-\varepsilon)}{1-\rho_{\text{g}}(1-\varepsilon)}, \tag{5}$$

where ρ_{g} is the reflectance of the gold and ε is the emissivity of the target surface. If $\rho_{\text{g}} = 1$ or $\varepsilon = 1$, then the effective emissivity of the surface is also 1. In practice, of course, neither of these conditions holds, but nevertheless, significant enhancement in the effective emissivity is achieved. In a smooth polished condition, gold has a reflectance of around 0.98 in the infrared, so for a surface of emissivity $\varepsilon = 0.2$, its effective emissivity becomes $\varepsilon_{\text{eff}} = 0.926$. Typically, though, in an industrial environment, the gold surface quickly becomes tarnished, lowering its reflectance and making the reflectance somewhat variable with time.

Accurate temperature measurement thus requires knowledge of the effective emissivity, given by Eq. 5, for the particular measurement conditions. That is, the effective emissivity cannot be assumed to be 1. The uncertainty in ε_{eff} due to uncertainties in ρ_{g} and ε is

$$u_{\varepsilon_{\text{eff}}} = \frac{\left[\left(\varepsilon(1-\varepsilon)u_{\rho_{\text{g}}}\right)^2 + \left((1-\rho_{\text{g}})u_{\varepsilon}\right)^2\right]^{1/2}}{\left[1-\rho_{\text{g}}(1-\varepsilon)\right]^2}. \tag{6}$$

To determine how this propagates to a measured temperature, Eq. 2 can be used with ε replaced by ε_{eff}. Assuming a degraded value of reflectance of the gold, due to tarnishing, of $\rho_g = 0.9$, and uncertainties of $u_{\rho_g} = 0.06$ and $u_\varepsilon = 0.06$, Eq. 6 gives $u_{\varepsilon_{\text{eff}}} = 0.14$, and Eq. 2 gives $u_{T_m} = 14°\text{C}$ at a temperature of 520 °C for a wavelength of 1.6 μm. While this is an improvement over the methods discussed above, problems associated with the use of the device, including the necessity of holding the gold cup above a moving surface (rather than in contact with it) and possible contamination of the window at the top of the hemisphere, lead to larger uncertainties. Furthermore, gold-cup pyrometers often operate over very wide bandwidths. In the case of a T^4 response, an uncertainty of $u_{\varepsilon_{\text{eff}}} = 0.14$, as determined above, leads to $u_{T_m} = 40\,°\text{C}$ at a target temperature of 520 °C.

3 "Disappearing Object" Thermometer

The proposed "disappearing object" thermometer is designed to minimize the dependence of the measured temperature on reflected radiation and, in particular, emissivity. This is achieved by enclosing the target in a blackbody cavity, with open ends to allow movement of the product through the cavity. The main components of the proposed thermometer are shown in Fig. 2. They comprise:

- *Radiation thermometer*: this would normally be a conventional spectral-band thermometer (either permanently mounted or a hand-held device), a thermal imaging system, or a fiber-optic device.
- *Temperature-controlled cavity*: this would ideally be of high thermal conductivity (e.g., a heat pipe) so that it is very uniform in temperature, and have a high internal surface emissivity. The cavity could be a cylinder, as drawn in Fig. 2a, for extrusion applications, a flat plate, as in Fig. 2b, for a steel strip mill, or some other shape appropriate to the application.

Two key requirements are that the cavity should occupy a large fraction of the hemisphere above the area of the target viewed by the thermometer, and that during operation, the cavity wall should be controlled to the desired process temperature. Thus, Eq. 1 is applicable, where T_w now represents this desired process temperature.

A simple rearrangement of Eq. 1 serves to illustrate the utility of this approach;

$$L_b(\lambda, T_s) = L_b(\lambda, T_w) + \frac{L_b(\lambda, T_m) - L_b(\lambda, T_w)}{\varepsilon(\lambda)}, \tag{7}$$

where L_m has been written as $L_b(\lambda, T_m)$, with T_m the radiance temperature measured by the thermometer when aimed at the target (i.e., the instrumental emissivity is set to 1). Thus, when the measured temperature T_m is equal to T_w, the true temperature T_s is also equal to T_w regardless of the value of the emissivity. On the other hand, when the true temperature is close to the desired process temperature (i.e., T_m, T_s, and T_w are all similar), Eq. 7 can be approximated by

$$T_s = T_w + \frac{T_m - T_w}{\varepsilon(\lambda)}. \tag{8}$$

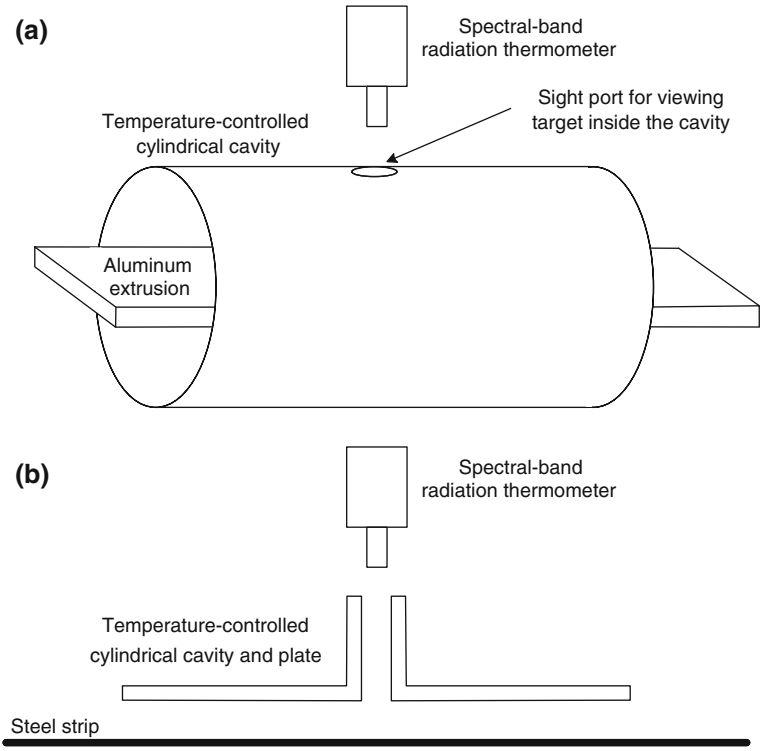

Fig. 2 Simplified schematics of the proposed "disappearing object" thermometer. Configuration in (**a**) could be used in an aluminum extrusion plant, and that in (**b**) in a steel strip mill

This equation clearly demonstrates the operating principle of the disappearing object thermometer: the temperature of the target is inferred from a temperature measurement of the cavity, a radiance temperature measurement of the target, and an estimate of its emissivity. The cavity temperature would normally be measured with a contact probe, such as a thermocouple or platinum resistance thermometer, embedded into the cavity wall close to its inside surface. Equation 8 also shows that the estimate of emissivity only impacts on a small measured temperature difference rather than directly on the measured temperature, as in conventional radiation thermometry or, to a lesser extent, gold-cup thermometry.

The degree to which Eq. 8 approximates Eq. 7 improves as the operating wavelength becomes longer, as shown in Fig. 3, and for low emissivities, is only valid when T_m is within a few degrees of T_w. In fact, because the low emissivity of the surface implies a high reflectance, most of the measured signal is due to radiation emitted by the cavity, not the target. Figure 4 illustrates that the measured temperature, T_m, does not change significantly for wide changes in the true target temperature, T_s. Thus, Eq. 7, not Eq. 8, must be used to predict the target temperature when it is not close to the cavity temperature.

When the target temperature is close to the desired process temperature, the uncertainty in the estimated temperature can be derived from Eq. 8;

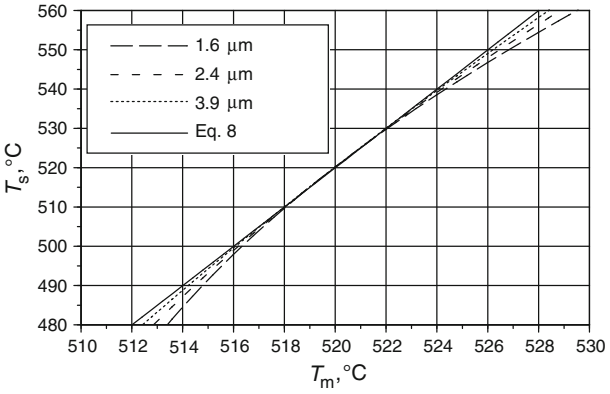

Fig. 3 Relationship between measured temperature, T_m, and true target temperature, T_s, as given by Eq. 7, for the disappearing object thermometer with a cavity temperature of $T_w = 520\,°C$ measuring a target, near this desired temperature, whose emissivity is $\varepsilon(\lambda) = 0.2$. *Solid line* is the approximation of Eq. 8

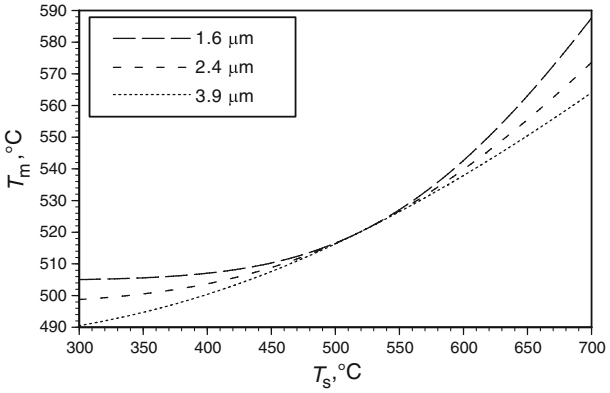

Fig. 4 Measured temperature for the disappearing object thermometer as a function of true target temperature for a cavity temperature of 520 °C and target emissivity of 0.2. For such low emissivities, most of the measured signal is due to reflections from the cavity wall, so the thermometer reads close to the cavity temperature even when the target temperature is significantly lower

$$u_{T_s}^2 = \frac{1}{\varepsilon^2} u_{T_m}^2 + \frac{(1-\varepsilon)^2}{\varepsilon^2} u_{T_w}^2 + \frac{(T_s - T_w)^2}{\varepsilon^2} u_\varepsilon^2, \tag{9}$$

where the wavelength dependence of $\varepsilon(\lambda)$ has been omitted for clarity. When the target and cavity temperatures are the same, the thermometer is insensitive to the uncertainty in the emissivity, otherwise, the total uncertainty obtains a minimum close to where this condition holds. In Fig. 5, each component of uncertainty, derived from the full Eq. 7 [10], rather than using the approximation of Eq. 9, is plotted for a wide range of T_w values for a target at $T_s = 520\,°C$. This figure demonstrates the small window of T_w values where the total uncertainty is largely insensitive to the uncertainty in emissivity. The disappearing object thermometer exploits this window by controlling the temperature of the surroundings.

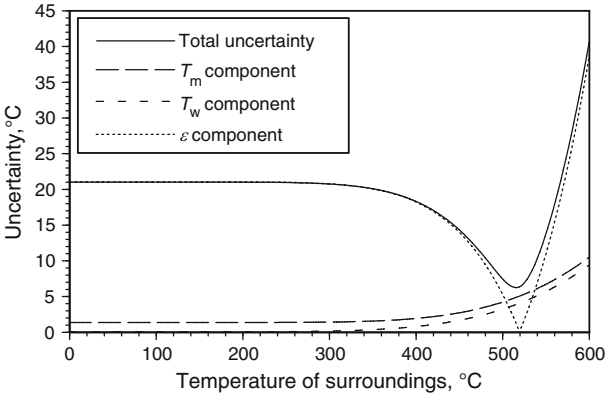

Fig. 5 Total uncertainty in target temperature, and each contributing component, after applying corrections for reflection errors, as a function of the temperature of the surroundings. The true target temperature is 520 °C, the uncertainties in the measured target temperature, T_m, and the measured temperature of the surroundings, T_w, are both 1 °C, and the uncertainty in emissivity is 0.06 °C. The target temperature measurement is made using a 1.6 μm radiation thermometer

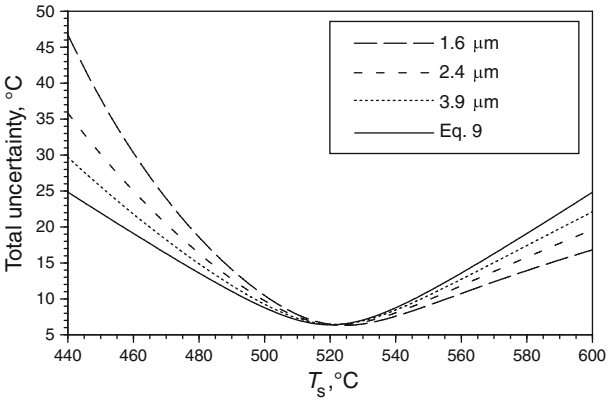

Fig. 6 Uncertainty in true target temperature for calculations based on Eq. 7 using measurements of T_m and T_w and an estimate of $\varepsilon(\lambda)$. *Solid curve* is the uncertainty given by Eq. 9, which is based on the approximation of Eq. 8. It is assumed that $T_w = 520$ °C with an uncertainty of 1 °C, the uncertainty in T_m is also 1 °C, and the emissivity is 0.2 with an uncertainty of 0.06

Figure 6 plots the total uncertainty for typical conditions in an aluminum extrusion plant for the three wavelengths chosen previously. Again, these curves have been derived from the full Eq. 7. The approximation of Eq. 9 is also plotted as the solid curve as a comparison. When the target is close to the desired temperature, the uncertainty is about 6.4 °C independent of wavelength, which is considerably smaller than that for the other radiation thermometry approaches discussed above. For the galvannealing application, where the emissivity may vary from 0.1 to 0.8, the emissivity can be assumed to be 0.45 with a standard uncertainty of 0.2 (assuming a rectangular distribution). In this case, the minimum uncertainty drops to about 2.5 °C. On the other hand, for conventional radiation thermometry, the uncertainty is increased in line with

Eq. 2, since the ratio $u_\varepsilon/\varepsilon$ increases from 0.3 for the aluminum application to 0.45 for galvannealing.

3.1 End Effects

Because the cavity must necessarily be open-ended to allow the product to pass through, it does not form a true blackbody. Thus, the temperature of the cavity wall, T_{cav}, measured by the contact thermometer, is not equal to the radiance temperature T_{w} appearing in Eqs. 7–9. As mentioned previously, T_{w} is the weighted average radiance temperature of the complete hemisphere above the target spot, including the open ends of the cavity. These ends, through which the product passes, will have a different temperature to that of the cavity wall, so that the average temperature of the surroundings will differ from the true cavity wall temperature. Additionally, if the cavity wall is not black, then this modifies further the relationship between T_{w} and T_{cav}. If the measured value of T_{cav} is used in Eq. 7 or 8 in place of T_{w}, then an error will occur in the calculated value of T_{s}. Ideally, the end effects should be small enough that the difference between T_{w} and T_{cav} is significantly smaller than the uncertainties plotted in Fig. 6, in which case T_{cav} would be a good representation of T_{w}.

3.1.1 Black Cavity

To determine the $T_{\mathrm{cav}} - T_{\mathrm{w}}$ difference, it will be assumed in the first instance that the cavity is black, that the open ends can also be considered black, and that there are no other surfaces at any other temperature in the hemisphere above the target spot. In this case, the quantity $L_{\mathrm{b}}(\lambda, T_{\mathrm{w}})$ in Eq. 7 is given by the weighted sum of the blackbody radiance of the cavity wall and the blackbody radiance of the open ends:

$$L_{\mathrm{b}}(\lambda, T_{\mathrm{w}}) = g_{\mathrm{cav}} L_{\mathrm{b}}(\lambda, T_{\mathrm{cav}}) + (1 - g_{\mathrm{cav}}) L_{\mathrm{b}}(\lambda, T_{\mathrm{amb}}), \tag{10}$$

where T_{amb} is the temperature of the open ends, assumed to be the ambient temperature for the aluminum extrusion application and the temperature of the annealing furnace for the galvannealing application. The quantity g_{cav} is the geometric view factor for the cavity wall as seen from the measurement spot. If the cavity were to fill the whole hemisphere above the target, then g_{cav} would equal 1 and T_{w} would equal T_{cav}. However, as the cavity becomes smaller, more of the open end is viewed from the measurement spot and T_{w} moves away from T_{cav} towards T_{amb}.

Two cases are considered here for the calculation of g_{cav}. The first is for the geometry shown in Fig. 2a, where a flat rectangular product is passing through the center of a cylindrical cavity. The cavity has length L and radius R. By using the methods outlined in [11], and ignoring the influence of the small viewing port for the radiation thermometer, it can be shown that

$$g_{\mathrm{cav}} = \frac{2\left[2f + (4 + f^2)\tan^{-1}(f/2)\right]}{\pi(4 + f^2)}, \tag{11}$$

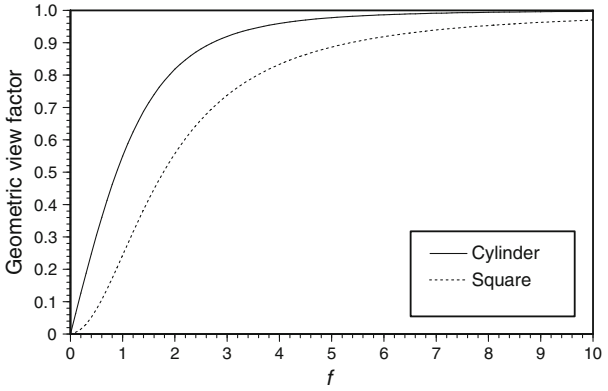

Fig. 7 Geometric view factors given by Eq. 11 for a cylindrical cavity (*solid curve*) and Eq. 13 for a square flat-plate cavity (*dotted line*). For the cylindrical cavity the horizontal axis, f, is the length-to-radius ratio, and for the flat plate f is the ratio of the plate length to target–plate separation

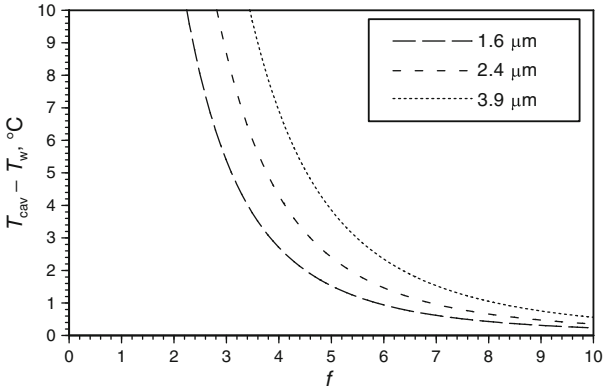

Fig. 8 Difference between the true cavity wall temperature and the average wall radiance temperature (T_w in Eq. 7) as a function of the length-to-radius ratio for a cylindrical cavity. The cavity wall is assumed to be black and at a temperature of $T_{cav} = 520\,°C$, while the open ends of the cylinder are at 20 °C

where $f = L/R$. This function is plotted as the solid curve in Fig. 7, and the difference $T_{cav} - T_w$, determined by Eq. 10, is plotted in Fig. 8 as a function of f for values of $T_{cav} = 520\,°C$ and $T_{amb} = 20\,°C$. In order for this difference to be less than, say, 1 °C, the value of f must be greater than about 8, in the worst case of a 3.9 μm thermometer. The radius would be determined from the maximum extrusion width that the device would need to accommodate. For example, a maximum width of 300 mm would imply $R = 150$ mm and, thus, a cavity length of at least $L = 1200$ mm would be required to keep the end effects below 1 °C. For a thermometer operating at 1.6 μm, the length would only need to be $L = 900$ mm for the same end effect.

The second geometry is for a rectangular product passing beneath a parallel rectangular flat plate (Fig. 2b) whose width is W and length is L. The plate is a distance R above the target. In this case, again ignoring the viewing port for the radiation thermometer,

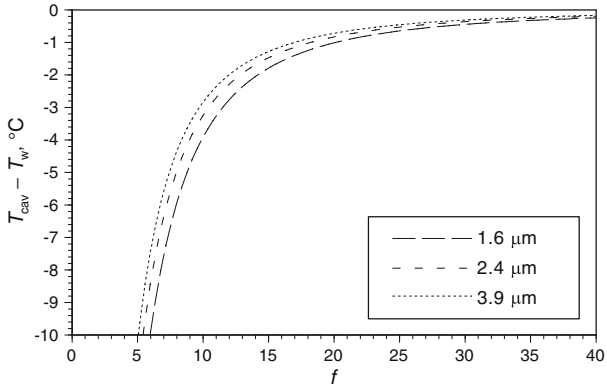

Fig. 9 Difference between the true cavity wall temperature and the average wall radiance temperature (T_w in Eq. 7) as a function of the length-to-separation ratio for a square flat-plate cavity. The plate's surface is assumed to be black and at a temperature of $T_{cav} = 520\,°C$, while the four open ends of the cavity, formed by the plate and the product, are at 600 °C

$$g_{cav} = \frac{2}{\pi}\left[\frac{f_W \tan^{-1}\left(\frac{f_L}{\sqrt{4+f_W^2}}\right)}{\sqrt{4+f_W^2}} + \frac{f_L \tan^{-1}\left(\frac{f_W}{\sqrt{4+f_L^2}}\right)}{\sqrt{4+f_L^2}}\right], \tag{12}$$

where $f_L = L/R$ and $f_W = W/R$. If the plate is square ($f_W = f_L = f$), then this reduces to

$$g_{cav} = \frac{4f}{\pi\sqrt{4+f^2}} \tan^{-1}\left(\frac{f}{\sqrt{4+f^2}}\right). \tag{13}$$

This is plotted as the dotted curve in Fig. 7, and the difference $T_{cav} - T_w$ is plotted in Fig. 9 as a function of f for values of $T_{cav} = 520\,°C$ and $T_{amb} = 600\,°C$. In this case, T_{amb} is taken to be the temperature of the annealing furnace, which is assumed to be uniform as seen through all four open gaps between the plate and the product. Clearly, a square plate is the worst case scenario, but increasing the length only marginally reduces the $T_{cav} - T_w$ difference. For the end effects to be less than 1 °C, for a 3.9 μm thermometer the value of f would need to be at least 17. Thus, if the plate were positioned $R = 50$ mm above the target, the length of the plate would need to be at least $L = 850$ mm. At 1.6 μm, the f value would need to be at least 20, implying a plate length of at least $L = 1000$ mm.

3.1.2 Non-black Cavity

If the emissivity of the cavity wall is less than 1, then the relationship between T_{cav} and T_w is more complicated than that given by Eq. 10. Because the cavity wall now reflects radiation, as well as emitting it, the equation for T_w becomes a function of the

emissivities of each surface seen from the cavity wall (including the product itself) and the true temperatures of each surface. Methods given in [11] can be used to produce a set of simultaneous integral equations for the radiant fluxes leaving each surface, from which the quantity $L_b(\lambda, T_w)$ can be determined. The geometries of both the cylinder and the flat plate are sufficiently complex that numerical methods are needed to solve these integral equations. These calculations are beyond the scope of this article, but will be the subject of future work to extend the analysis presented above to non-black cavity walls.

However, it is pointed out here that if the inside of the cavity is measured directly with a radiation thermometer operating at the same wavelength as the thermometer viewing the target, then T_w corresponds directly to this measured radiance temperature. A complication with this is that, even if the cavity surface is isothermal, each part of the cavity wall will have a different radiance temperature due to its relative location with respect to the other surfaces. In practice, the cavity would need to be sampled fully and a weighted average determined. This sampling could be streamlined by using a thermal imaging camera. On the other hand, physical constraints may make it impossible to position a radiation thermometer so that it can view a significant portion of the cavity wall.

4 Conclusions

In this article, a new type of radiation thermometer (described here as the "disappearing object" thermometer) has been proposed to overcome problems associated with the temperature measurement of low-emissivity metals in industrial processes. The thermometer uses blackbody principles to effectively enhance the emissivity of the target to a value close to 1. While a prototype of this thermometer has not yet been constructed, the uncertainty analysis based on the design principles indicates that it should be capable of considerable improvement in accuracy over existing methods.

The proposed thermometer is ideally suited to process-control applications, where the controller would drive the target to meet the $T_s = T_w$ criterion, which minimizes the uncertainty in the measurement. In this case, the blackbody can be maintained at a single temperature. For general purpose applications, the disappearing object thermometer would require a temperature-controlled cavity that is servo-controlled to the observed temperature, and the cavity would be required to have a relatively fast response.

Table 1 compares the performance of the current radiation thermometry methods with that of the proposed thermometer. For the purposes of comparison, it is assumed that the operating wavelength of the radiation thermometers is near 1.6 μm, that radiance temperatures (and cavity temperature for the disappearing object thermometer) can be measured with an uncertainty of 1 °C, and that the emissivity of the metal surface is 0.2 with an uncertainty of 0.06 (aluminum extrusion application). The table demonstrates the improvement in performance of the disappearing object thermometer over other current methods. The disappearing object thermometer also performs extremely well for other applications, such as galvannealing.

Table 1 Comparison of the performance of various types of radiation thermometers for an aluminum extrusion application

Thermometer type	Typical uncertainty (°C)	Comments
Conventional spectral-band	>21	Best case when there are no reflections. Limited by emissivity uncertainty
Ratio	>40	Assumes $\varepsilon(\lambda_1) = \varepsilon(\lambda_2)$
Compensated ratio	20	Applies to one alloy only
Multi-wavelength	100	Assumes no prior knowledge of emissivity
Smart multi-wavelength	20	Assumes correct identification of alloy
Gold cup	>14	Assumes correction applied for effective emissivity. Difficult to use in practice
Disappearing object	6.4	Near process temperature only

All uncertainties are standard uncertainties

Two possibly important factors have been omitted from the calculations presented here. The first is the effect of a non-black cavity surface, which has already been mentioned. The second is the effect of specular reflections on the measured temperature. These may in fact lower the end effects over those calculated above for purely diffuse reflectance, so long as the cavity occupies all of the solid angle from where specular reflections originate. Measurements of the bi-directional reflectance distribution function of metals could be used to model these end effects. Whether or not these two effects are significant, it is expected that the only factor affecting the final accuracy would be the required length of the cavity.

References

1. P.G. Cielo, J.C. Krapez, M. Lamontagne, J.G. Thomson, M.G. Lamb, *Conical-Cavity Fiber Optic Sensor for Temperature Measurement in a Steel Furnace*, SPIE, vol. 1682 (Thermosense XIV, 1992), pp. 142–154
2. J.C. Krapez, C. Bélanger, P. Cielo, Meas. Sci. Technol. **1**, 857 (1990)
3. M.D. Drury, K.P. Perry, T. Land, J. Iron Steel Inst. **169**, 145 (1951)
4. T. Yamada, E. Makabe, N. Harada, K. Imal, *Development of Radiation Thermometry Using Multiple Reflection*, *Nippon Kokan Tech. Rep.*, Overseas No. 41 (1984)
5. I. Ridley, T.G.R. Beynon, Measurement **7**, 171 (1989)
6. G.R. Peacock, in *Temperature: Its Measurement and Control in Science and Industry*, vol. 7, ed. by D.C. Ripple, B.C. Johnson, C.W. Meyer, R.D. Saunders, G.F. Strouse, W.L. Tew, B.K. Tsai, H.W. Yoon (AIP, New York, 2003), pp. 789–794
7. D.P. DeWitt, G.D. Nutter, *Theory and Practice of Radiation Thermometry* (John Wiley & Sons, New York, 1988)
8. Y.S. Touloukian, D.P. DeWitt, *Thermophysical Properties of Matter*, vol. 7 (IFI Plenum, New York, 1970)
9. L.K. Zentner, D.P. DeWitt, D.A. White, D.R. Gaskell, in *Temperature: Its Measurement and Control in Science and Industry*, vol. 6, ed. by J.F. Schooley (AIP, New York, 1992), pp. 861–864
10. P. Saunders, in *Radiation Thermometry: Fundamentals and Applications in the Petrochemical Industry* (SPIE Press, Bellingham, Washington, 2007)
11. R. Siegel, J.R. Howell, *Thermal Radiation Heat Transfer*, 4th edn. (Taylor & Francis, New York, 2002)

12. P. Saunders, in *Proceedings of TEMPMEKO '99, Seventh International Symposium on Temperature and Thermal Measurements in Industry and Science*, ed. by J.F. Dubbeldam, M.J. de Groot (Edauw Johannissen bv, Delft, 1999), pp. 631–636
13. L. Michalski, K. Eckersdorf, J. McGhee, *Temperature Measurement* (John Wiley & Sons, London, 1991)
14. P. Saunders, High Temp.-High Press. **32**, 239 (2000)
15. P.B. Coates, High Temp.-High Press. **20**, 433 (1988)